Int J Adv Manuf Technol (2017) 93:651–660
DOI 10.1007/s00170-017-0508-6

ORIGINAL ARTICLE

# Investigation on performance characteristics in drilling of Ti6Al4V alloy

**Zhaoju Zhu [1,2] · Shaochun Sui [3] · Jie Sun [1,2] · Jianfeng Li [1,2] · Yanle Li [1,2]**

Received: 25 October 2016 / Accepted: 2 May 2017 / Published online: 24 May 2017


**Abstract** Titanium alloys are attractive materials for aerospace, biomedical and chemical engineering due to their excellent combined performance of high specific strength and fracture resistant characteristics. Drilling titanium alloys is essential to the bolted/rivet connection in the assembly of aerospace parts. This paper outlines a comprehensive analysis of drilling characteristics and hole quality/integrity assessment following drilling titanium alloy Ti6Al4V without coolant under different machining parameters. The experimental results show that hole quality can be improved by proper selection of cutting parameters. This is substantiated by monitoring thrust force, hole diameter, circularity, chip formation, and surface finish. It was observed that the thrust force increased rapidly with respect to feed rate, which was increased by 2.5 times when the feed was increased from 0.05 to 0.13 mm/r as a constant cutting speed of 40 m/min. In addition, the circularity was found to be around 4 μm at low feed rate, when the feed was increased the circularity increased to 10 μm. The experimental results also indicated that the shape and the size of chips were strongly influenced by feed rate. Observation on the subsurface of drilled workpiece indicated a severe plastic deformation under different cutting conditions. This study demonstrates that using proper process parameters plays an important role in improving machining efficiency and guaranteeing quality in dry drilling titanium alloy.

**Keywords** Drilling · Titanium alloy · Performance characteristics · Chip · Microstructure

✉ Jie Sun
sunjie@sdu.edu.cn

[1] School of Mechanical Engineering, Shandong University, Jinan 250061, China

[2] Key Laboratory of High Efficiency and Clean Mechanical Manufacture, Ministry of Education, Shandong University, Jinan 250061, China

[3] AVIC Cheng Du Aircraft Industrial (Group) Co., Ltd., Chengdu, China

## 1 Introduction

Used in a very large variety of applications including aeronautical and automotive industries for structural assembly, drilling is one of the most complex manufacturing processes. Drilling is also regarded as an important machining process due to the fact that it is involved in nearly all titanium alloy applications [1].

Titanium alloys cover an increasingly wide variety of applications in aerospace, chemical processing, biomedical, automotive, and nuclear industries owing to their outstanding combination of high specific strength (strength-to-density ratio), fracture resistant characteristics, and general corrosion resistance. For example, on Boeing 787, the utility of titanium alloys has been expanded to roughly 14% of the total airframe [2]. However, titanium alloys are regarded as difficult-to-machining materials because of their high strength at elevated temperature, relatively low modulus of elasticity, low thermal conductivity, high chemical activity, and small deformation coefficient [3–7].

A large amount of research has been carried out in drilling titanium alloy Ti6Al4V with respect to thrust force, tool wear, and hole quality. Cantero et al. [8] conducted an experimental observation on the evolution of tool wear, quality of machined holes, and surface integrity of workpiece in the dry drilling of titanium alloy Ti6Al4V. A large amount of experiments of high-throughput drilling of titanium alloy Ti6Al4V were conducted by Rui Li and Albert [9]. They aimed to evaluate the effect of tool material, geometry, and drilling process

**Table 1** Chemical composition of Ti6Al4V

| Element | Ti | Al | V | Fe | C | N | H | O |
|---|---|---|---|---|---|---|---|---|
| Wt% | Base | 5.5–6.75 | 3.5–4.5 | <0.25 | <0.08 | <0.05 | <0.01 | <0.2 |

swarf morphology. Denkena et al. [16] showed that the quality of the holes could be increased by helical milling of CFRP-Ti stacks. Kim et al. [17] stated that the optimum process conditions for achieving desired hole quality and process cost while drilling Gr/Bi-Ti are the combination of low speed and low feed when using carbide drills and low speed and high feed in drilling with HSS-Co drills. Pawar et al. [18] compared the wear of coated carbide drills in drilling of Ti, CFRP, and CFRP/Ti stacks separately and analyzed the effect of chip flow on hole surface quality. Bono and Ni [19] established a finite element model and experimental investigation of the effects of thermal distortions on the diameter and cylindricity of dry drilled holes. They found that thermal expansion of the drill was the dominant effect and led to oversized holes with diameters that increased with depth. In addition, quantitative analysis of chip extraction in drilling of Ti6Al4V has been investigated by Brinksmerier et al. [20]. Prasanna et al. [21] conducted an experiment on optimization of process parameters of small hole dry drilling in Ti6Al4V using Taguchi and gray relational analysis. The outcome of his research revealed that spindle speed has the most significant impact on the dimensional accuracy of drilled hole. Besides, some researchers focused on the analysis of burr formation in drilling process [22–24].

**Table 2** Physical property of Ti6Al4V

| Parameter | Value | Parameter | Value |
|---|---|---|---|
| Density/(kg/m$^3$) | 4430 | Area reduction/% | 14.0 |
| Melting point/°C | 1668 | Yield strength/MPa | 820 |
| Thermal conductivity/(W/m°C) | 7.3 | Young's modulus/GPa | 113.8 |
| Ultimate strength/MPa | 950 | Poisson's ratio | 0.342 |
| Specific heat/(J/(kg/°C)) | 526 | | |

parameters on drill life, thrust force, torque, energy, and burr formation. Dornfeld et al. [10] showed that both feed rate and cutting speed had limited influence on burr size when drilling Ti6Al4V, although this could be attributed to the restricted range of cutting speed (6–10 m/min) and feed rate (0.04–0.20 mm/r) levels employed in these experiments. Abdelhafeez et al. [11] implemented an experimental design based on response surface methodology to identify the effects of cutting speed and feed rate on burr size, hole diameter, and out of roundness as well as tool flank wear in drilling of titanium alloys Ti6Al4V. Cao et al. [12] conducted an investigation on monopulse electrical discharge machining ablation drilling technology for Ti6Al4V titanium alloy. Bermingham et al. [13] aimed to identify the advantages of milling and drilling Ti6Al4V components with high-pressure coolant. Bi and Liang [14] conducted a study on robotic drilling system for titanium structures instead of manual drilling. The results showed that the positional accuracy and the repeatability of system can be successfully placed. Soo et al. [15] conducted an investigation on hole quality assessment following drilling of metallic-composite stacks based on hole size, out of roundness, cylindricity, burr height, hole edge quality, average surface roughness, microhardness (of the metallic elements), and

Nevertheless, a comprehensive characterization of drilling titanium alloy Ti6Al4V and microstructural and mechanical behavior of drilled holes is significantly lacking. The research presented in this paper is focused on a systematic study of drilling performance, boreholes accuracy,

**Table 3** Drill information and cutting parameters

| Material | Tungsten carbide (WC-Co)-YG8 | | |
|---|---|---|---|
| Drill information | Tool diameter/mm | 3.6 mm | ,p) = " : 1 :: pdgts11747050800170 − 017 − 0508 − 6Fmca.tif" |
| | Flute | 2 flute | |
| | Point angle | 140° | |
| | Helical angle | 35° | |
| | Flute length/mm | 20 | |
| | Shank type | Cylindrical | |
| | Coating | Uncoated | |
| Cutting parameters | Cutting speed/m min$^{-1}$ | 26/40/55 | |
| | Feed rate/mm r$^{-1}$ | 0.05/0.13/0.2 | |

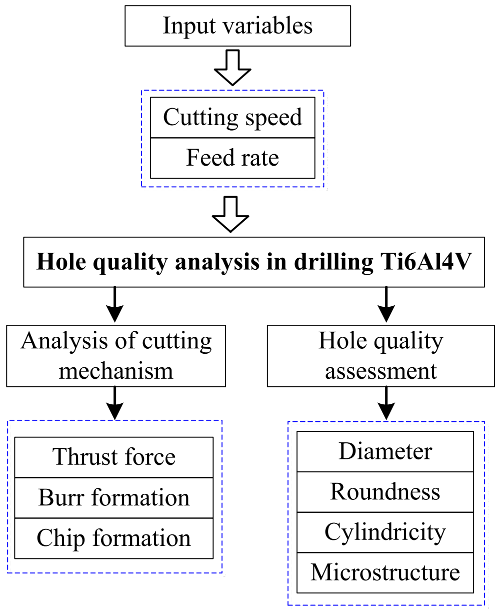


**Fig. 1** Theme of experimentation

and surface integrity of workpiece in drilling of titanium alloy Ti6Al4V.

## 2 Experimental procedures

### 2.1 Workpiece material and tool details

For the purpose of this trial, titanium alloys (Ti6Al4V) with chemical composition and physical property given in Tables 1 and 2 respectively were selected as the workpiece material according to [25]. Prior to beginning the drilling experiments, Ti6Al4V alloy sheets with 220 mm × 100 mm × 5 mm were selected based on the requirement of this trial. Solid carbide twist drill with 140 point angle and 35 helical angle without coating was used to drilling titanium alloy Ti6Al4V based on the literature, industrial applications, and tool manufacturer's recommendation. Table 3 details the dimensional information of the drilling tool (AHNO12041770036) and cutting parameters used in this research. The basic theme of experimentation is shown in Fig. 1. It includes an experimental set-up and a dynamometer for thrust force during drilling operation. The hole quality analysis includes diameter, roundness, cylindricity, and subsurface microstructure.

### 2.2 Experimental conditions

Drilling experiments were performed on DAEWOO ACE-V500 vertical machining center equipped with a 15 kW drive motor. The spindle motor provides a speed range from 80 to 10,000 rpm. The experiments were carried out without the use of coolant to have a clear view of the burr formation process and considering the impact of conventional cutting fluids on ecological environment. Figure 2 shows the schematic diagram of the experimental set-up with the data acquisition system. The thrust force was recorded using a Kistler 9257B dynamometer. The force signals were transmitted to a PC and analyzed using dynamometer software. Titanium alloy workpiece was clamped to a fixture, which was clamped to the faceplate of the dynamometer with bolt connection, prior to drilling. Four bearer supporting brackets were put under the workpiece plate to prevent the bending of workpiece plate. Voltage signals traveled through a commercial analog to digital I/O board, located inside a personal computer, where the

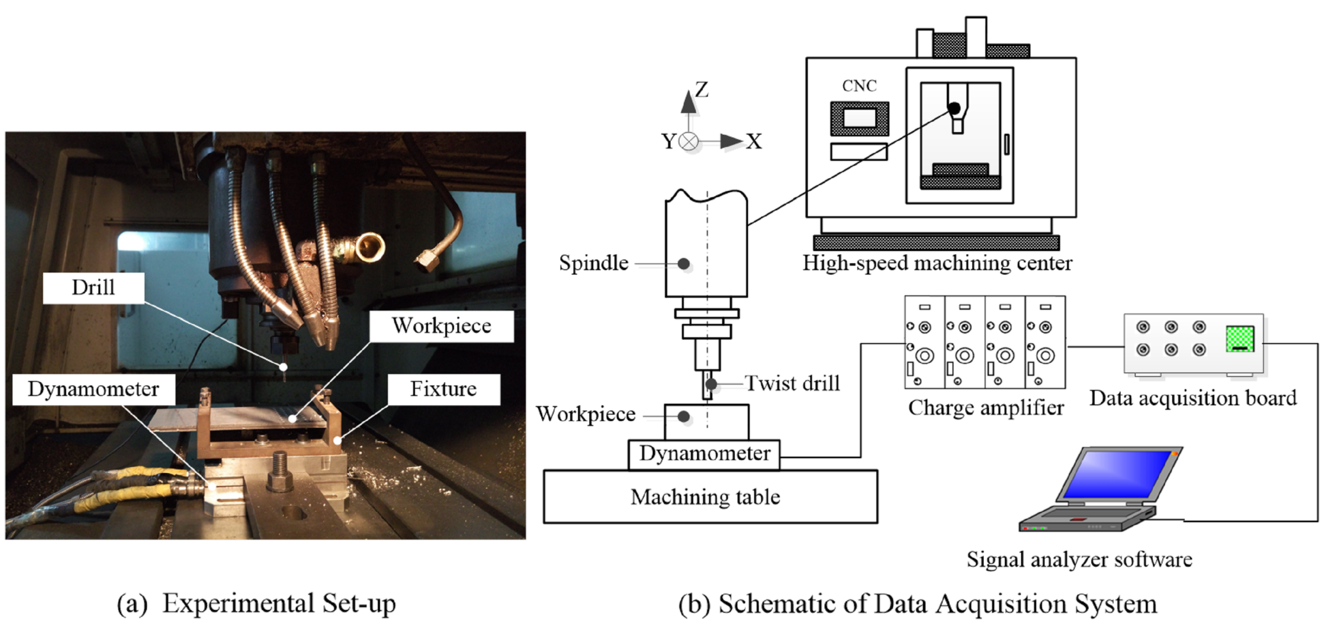


**Fig. 2** Experimental conditions. **a** Experimental set-up. **b** Schematic of data acquisition system

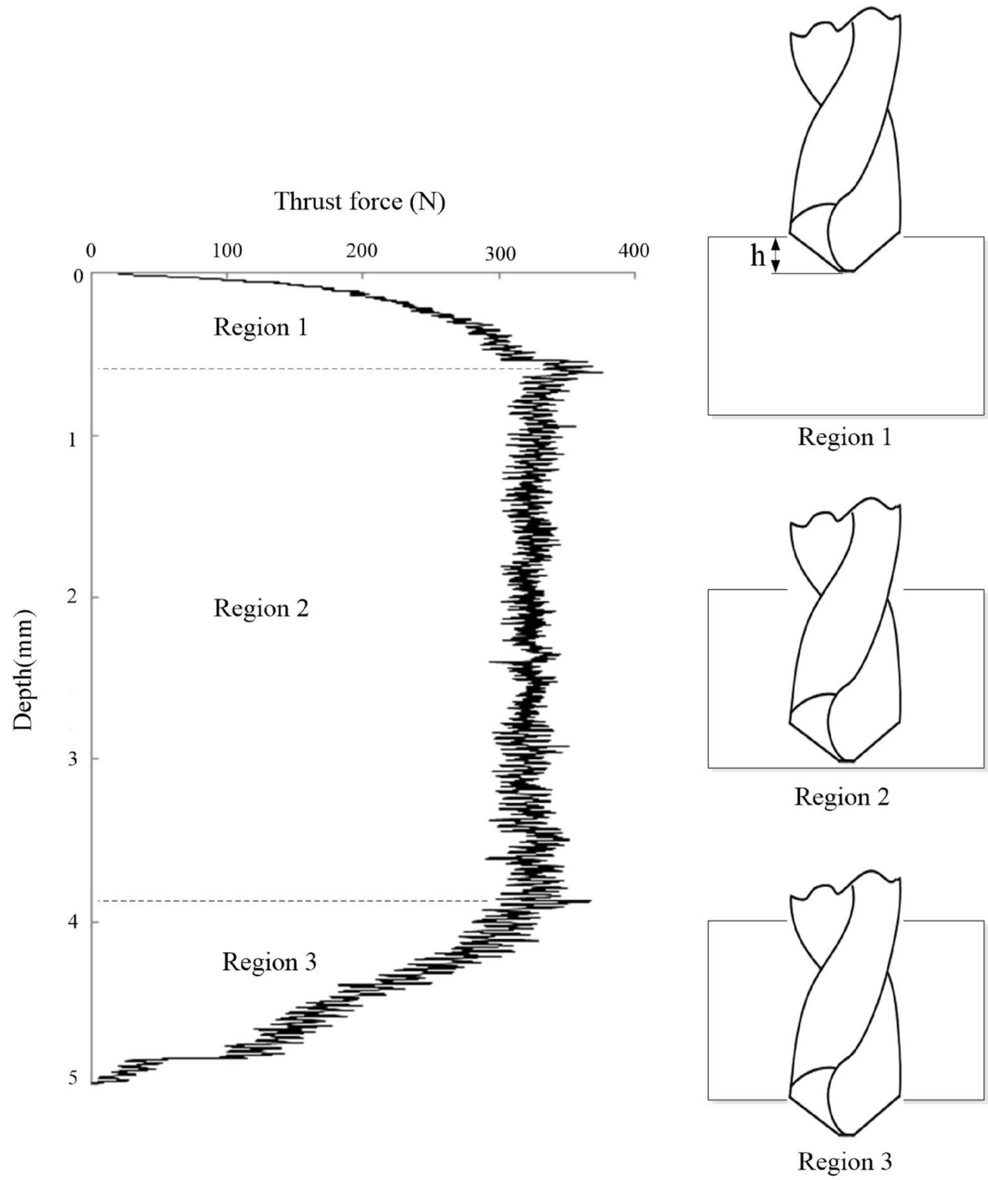


**Fig. 3** Thrust force and illustration of three regions 1, 2, and 3 in drilling

signal was converted to the digital domain. A customized software program was used to set the sampling frequency during the experiments and to display the output signals. Voltage data was recorded from the data acquisition system and post processed for further analysis.

In this study, the experiments were designed to investigate the influences of the cutting speed, feed rate on the cutting force, hole accuracy, chip formation, and surface integrity, respectively. Hole diameter, error of cylindricity, and roundness were measured using three coordinate measurement machine with a 1-mm-diameter ball probe. A series of measurements (replicated three times for each hole) was recorded and the average was computed. In order to study the reason of hole diameter variation, the residual stress on the surface of hole was measured by means of XStress3000 test system for three times. Both optical and scanning electron microscopy (SEM) were utilized to observe the drilled hole quality. The SEM was used to qualitatively assess the surface of drilling hole and to study the microstructure of each hole under different parameters. Surface formation and topography were characterized in terms of surface describing parameters through surface profile measurements. The surface roughness across depth of the hole walls was measured on Veeco-NT9300 System after the holes were cut in two parts.

## 3 Results and analysis

### 3.1 Analysis of thrust force

During drilling with cement carbide twist drill instead of cutting, the chisel edge of the drill point pushes aside the material

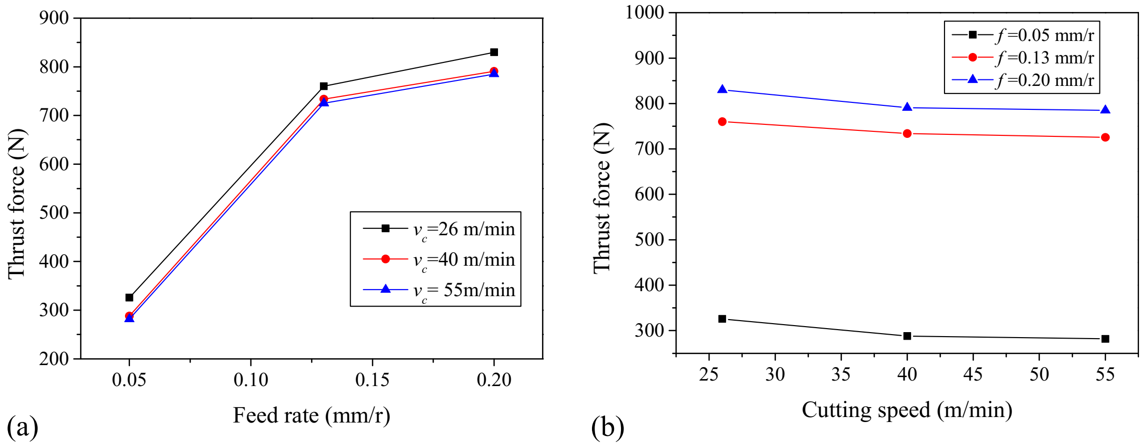


**Fig. 4** Evolution of the thrust force as a function of the **a** feed rate and **b** cutting speed

at the center as it penetrates into the hole. Figure 3 illustrates the variation curve of thrust force as a function of drilling depth measured during drilling titanium alloy Ti6Al4V at the cutting speed of 26 m/min and feed rate of 0.05 mm/r. It is noticed that there are three major regions in the thrust profiles during drilling. Region 1 defines the period when the drill has penetrated a distance *h*, which is equal to drill point length. For the twist drill used in this research, *h* is equal to 0.66 mm. As soon as the chisel edge enters the material, the thrust force increases rapidly and reaches the peek value (323 N) at the end of region 1. A constant thrust force occurred once the cutting edges of the drill were engaged in material, as shown in Region 2. However, the thrust force drops to zero in Region 3 when the drill cutting edge is disengaged with the workpiece. In addition, Young et al. [17] found that a positive thrust force may be observed after the drill exited the workpiece, resulting from burrs or chips stuck inside the hole.

Figure 4 represents the evolution of the thrust force recorded in drilling titanium alloy Ti6Al4V as a function of (a) feed rate and (b) cutting speed, respectively. It can be noted that each point represents an average value of three tests. From these average values of Fig. 4a, it can be observed that the thrust force during drilling titanium alloy Ti6Al4V increases rapidly with respect to feed rate. For example, when the feed increased from 0.05 to 0.13 mm/r as a constant cutting speed of 40 m/min, the force will also increase from 288 to 734 N. It increases approximately by 2.5 times. This is mainly due to the higher feed rate means the bigger material removal rate. However, from Fig. 4b, it can be noticed that the cutting speed has little influence on the thrust force. In addition, increasing cutting speed from 26 to 55 m/min is found to cause a slight decrease in the thrust force. This can be explained by the fact that increasing the cutting speed helps to raise temperature of machining due to the friction between the tool and titanium

**Fig. 5** Crack location in burr formation **a** crack at drill point before drill exits hole, **b** crack along the exit edge of the hole, **c** crack at drill point after drill exits hole, **d** burr with crack at drill point before drill exits hole, **e** burr with crack along the exit edge of the hole, and **f** burr with crack at drill point after drill exits hole

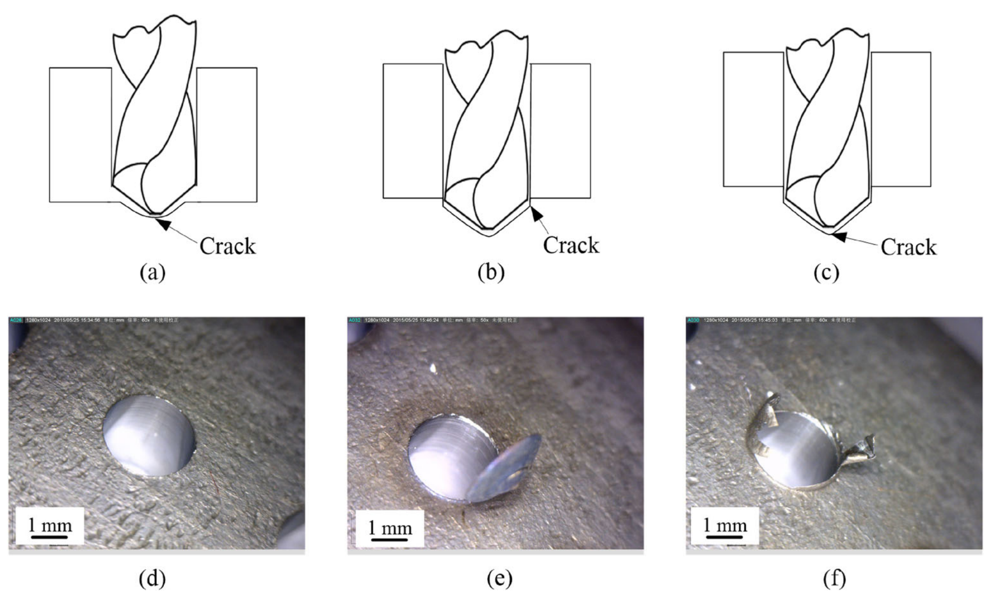

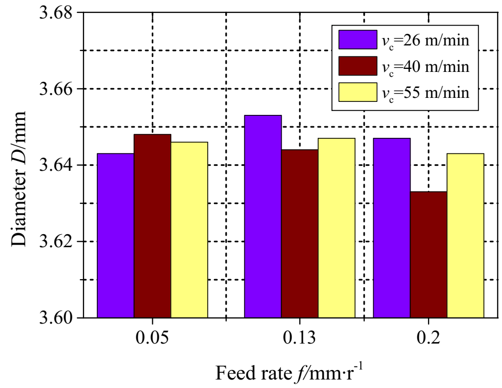


**Fig. 6** Hole diameter results for different cutting parameters

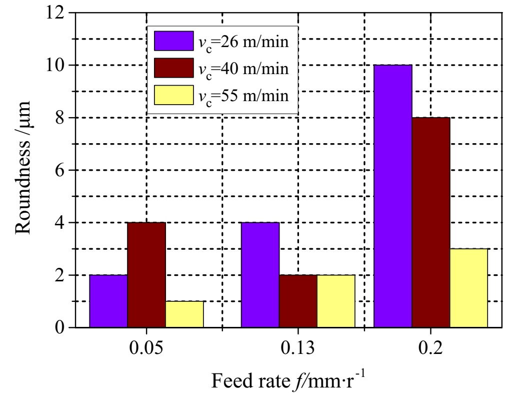


**Fig. 8** Roundness measurement results

alloy, thus resulting in softening of the material and a subsequent reduction in thrust force.

### 3.2 Burr formation mechanism

Burr formation in drilling is undesired in aerospace applications because of the difficulty of completely removing. It is estimated that up to 30% of the cost of typical components is due to deburring operations. Burrs are formed due to the plastic deformation and fracture at the exit stage of workpiece materials during drilling. The final morphology of the burr is determined by the amount of plastic deformation and the fracture strain of material. Therefore, the burr formation mechanism is decided by material properties.

There are three types of burr formation according to the fracture location during drilling from the results of previous analysis, as shown in Fig. 5. The fracture location is determined by comparing the strain at the drill point with that along the exit edge of the hole. When the twist drill approached the exit of the workpiece as shown in Fig. 5a, plastic deformation of the remaining material increased. Besides, the remaining material can be cut or be pushed out by thrust force. Under such drilling condition, when the material cannot sustain the plastic deformation, a crack was initiated at the drill point. Therefore, there were no or little burrs left on the exit of hole, as shown in Fig. 5d. If the plastic deformation continued after the drill exits the hole, two kinds of fracture may occur as shown in Fig. 5b, c. The one was cracked along the exit edge of the hole and the other one was from the drill point. The caps and burrs were formed uniformly, as shown in Fig. 5e. The part along the edge of the hole was subjected to tensile stress. If the fracture begins from the drill point, the cap can be torn into several pieces and remain as burrs which were large and irregular, as shown in Fig. 5f. Therefore, the burr formation type is determined by the initial crack location of the material which is depended on the ductility and fracture strain value. The size of burr is determined by the drill depth where the crack happens.

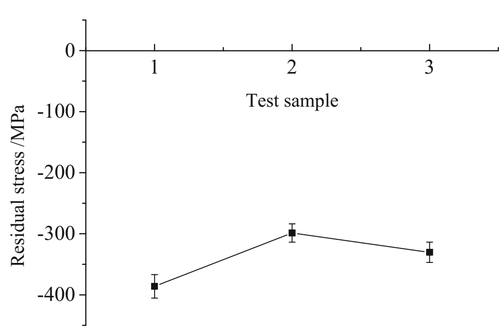


**Fig. 7** Residual stress for different test samples

### 3.3 Hole size and geometrical accuracy

Deviation of hole diameter is an important factor widely used to evaluate the quality and dimensional accuracy of drilled holes in industry. The effects of cutting speed and feed rate on hole diameter are complicated due to their interacting effects. On the one hand, the elastic recovery of compressive thermoplasticity produced by thrust force may decrease the hole size. On the other hand, a large amount of cutting heat can be produced during machining. The materials on the

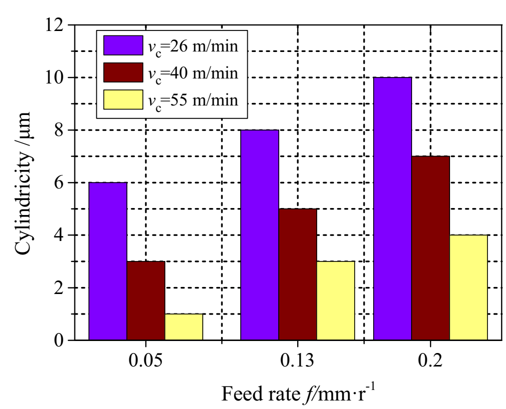


**Fig. 9** Cylindricity measurement results

**Fig. 10** Influence of the cutting speed and feed rate on titanium chips in dry drilling

| Cutting speed $v_c$ (m/min) | Feed rate $f$ (mm/r) | | |
|---|---|---|---|
| | 0.05 | 0.13 | 0.2 |
| 26 | 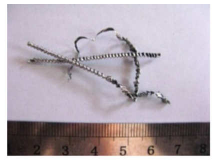 |  | 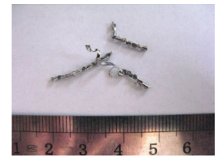 |
| 40 | 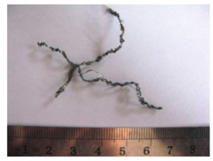 |  |  |
| 55 |  |  |  |

surface of hole begin to shrink after the drilling heat is dissipated based on the principle of thermal expansion and contraction which may increase the size of drilled hole.

Hole diameters for different cutting parameters and residual stress of three selected testing samples were depicted in Figs. 6 and 7, respectively. It can be seen from Fig. 6 that all hole diameters were oversized, and diameter errors ranged from 33 to 59 μm. This confirms the explanation that the heat generated by the process can lead to thermal expansion of the drill and workpiece, resulted in oversized holes. Therefore, it is clear that the effect from the expansion of drilling holes prevail over the effect from the contraction of the workpiece. In addition, Fig. 7 shows the residual stress for drilled holes and it was observed that values of all residual stress were negative. This meant that the drilling hole surface was subjected to compressive stress. This can also result in the oversized holes.

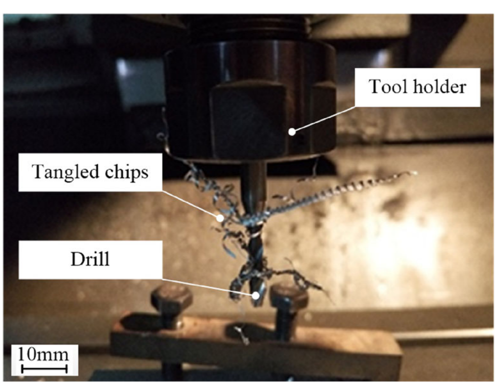


**Fig. 11** Tangled chips and hanging on the body of the tool at 26 m/min cutting speed and 0.05 mm/r feed in dry drilling titanium alloy Ti6Al4V

Roundness measurement provides information on hole shape, specifically for how the circular cross-section of a hole approximates to a true circle. Roundness of drilling hole is a two-dimensional geometric tolerance that permits how much a feature can deviate from a perfect circle, while cylindricity refers to the degree by which the entire cylinder deviates. Twelve points were measured located at different height (top, middle, and bottom) and orientation along the hole surface. The roundness and cylindricity measurement results are shown in Figs. 8 and 9. It can be seen from these figures that the maximum deviations in hole roundness and cylindricity were up to 10 μm under different cutting parameters (cutting speed and feed rate), respectively. Generally, values of hole roundness and cylindricity decrease with the increase of cutting speed with same feed rate. This demonstrates that the better hole quality can be obtained under the higher cutting speed. In addition, it can be observed that values of hole roundness and cylindricity decrease with the increase of cutting speed at the same feed rate. This can be explained by the fact that plastic deformation of workpiece material decreases with the progression of cutting speed. This results in the smaller hole roundness and cylindricity values under higher cutting speed.

### 3.4 Chip morphology analysis

Chip breakability is defined as the number of chips in 100 g of chip [26]. To break the chip into segments on possible solution would be to increase depth of the cut. However, the value of the depth of cut depends on cutting speed and feed rate. Figure 10 shows the typical macroscopic morphology analysis

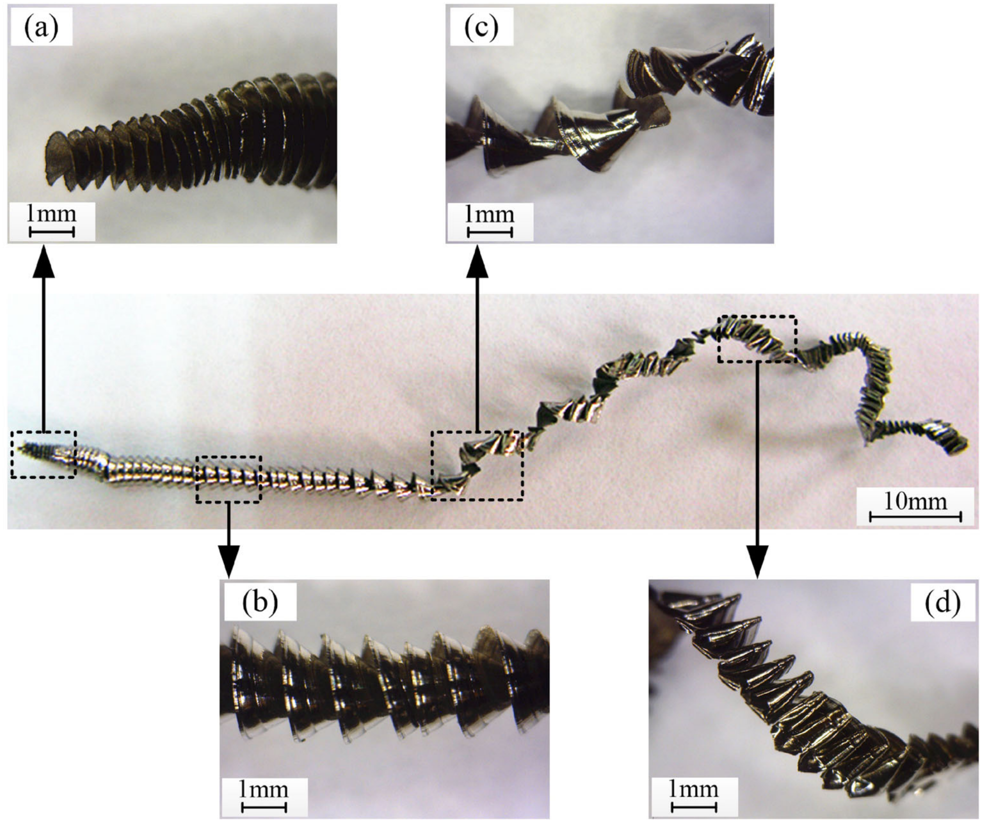


**Fig. 12** Chip morphology of titanium alloy Ti6Al4V at 26 m/min cutting speed and 0.05 mm/r in dry drilling. **a** Initial spiral cone. **b** Steady-state spiral cone. **c** Transition between spiral cone and folded long ribbon. **d** Folded long ribbon

of chips forming in drilling titanium alloy Ti6Al4V at different cutting speed and feed rate. It was noted that the shape and size of chips are strongly influenced by the feed rate. When the feed rate is greater or equal to 0.13 mm/r, chips are prone to be broken into small segments. For example, when the feed rate is increasing from 0.05 to 0.20 mm/r, the average chip length decreases from 60 to 20 mm. Increasing the feed rate favors formation of discontinuous chips. This may be due to the fact that the stiffness of the chip increases (the cross sectional area of chip increases) with feed rate. In this case, it is also seen that the effect of cutting speed on the shape and size of chips is less compared to the feed rate. The speed does not play any role in chip breakability and the chips of the same length are observed for all cutting speeds.

It is important to mention that the chips could be entangled around two flutes of the drill and bent by the tool holder when the feed rate is small ($f$ = 0.05 mm/r), as shown in Fig. 11. In this case, chips were found to be tangling on the body of the tool. This is called chip entanglement, which is due to the difficulty for smooth chip ejection. As we can see from Fig. 12, a continuous chip includes four regions as follows: (a) initial spiral cone, (b) steady-state spiral cone, (c) transition

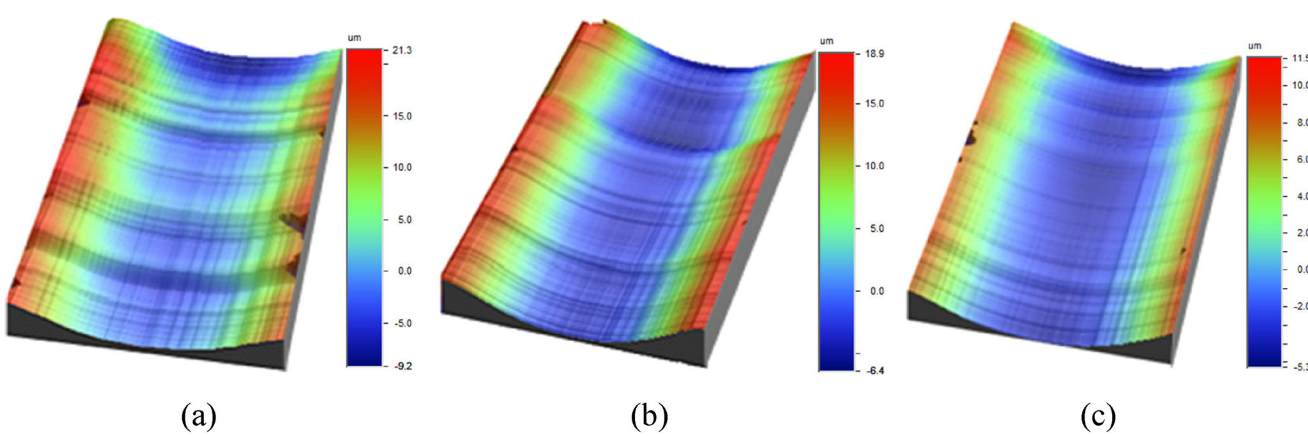


**Fig. 13** Topographic morphologies of drilling holes for different cutting parameters. **a** $v_c$ = 26 m/min, $f$ = 0.05 mm/r. **b** $v_c$ = 40 m/min, $f$ = 0.2 mm/r. **c** $v_c$ = 40 m/min, $f$ = 0.05 mm/r

between spiral cone and folded long ribbon, and (d) folded long ribbon. The initial spiral cone illustrated in Fig. 12a was generated at the start of drilling from the beginning of contact to Region 1. After Region 1, the steady-state spiral cone chip morphology, as shown in Fig. 12b, was generated. Due to the increased resistance to eject the chip, the spiral cone was changed to folded ribbon chip morphology. Close-up view of the chip transition region and the folded ribbon chip are shown in Fig. 12c, d, respectively. But in drilling titanium alloy, small well broken chips are desirable. This is because as the chips get larger, they cannot move easily through the flutes, which increases thrust force requirements and temperature, perhaps causing drill breakage.

### 3.5 Surface topography analysis

The surface topography is one of the main characteristics that has been tracked for evaluating cutting quality in machining processes. Figure 13 shows the surface topographic maps of a section of drilled hole. It can be seen from these maps that the hole quality was worst in the case with lowest cutting speed of 26 m/min and feed rate of 0.05 mm/r. The average surface roughness was 5.3 μm, and some parallel grooves were observed on the hole wall, as shown in Fig. 13a. The parallel grooves were reduced gradually with the increase of cutting speed and the decrease of feed rate, as shown in Fig. 13b, c. Their average surface roughness was 3.8 and 3.1 μm, respectively. This may be explained by the fact that the build-up edges and scales of hole surface were effectively restrained with the increase of cutting speed. Therefore, it can get better surface topography at high cutting speed and low feed rate.

Figure 14 depicts the surface microstructure of drilled holes under different cutting parameters. The images are a section of a hole containing the revolution axis of the drill. It can be observed that there are two distinct regions according to the feature of microstructure, named region A and region B. In region A which is closer to the drilled hole surface, the grains was refined obviously. This may be due to the high cutting temperature and squeezing action between hole surface and tool flank face. However, the grains presented different microstructure in region B. There was a strong distortion in this region, and the grains were oriented along the feed rate direction. In addition, plastic deformations during machining were caused by mechanical forces from the cutting tool acting upon the workpiece. It can also be observed that the influence on microstructure was more significant at high cutting speed 55 m/min and feed rate of 0.2 mm/r, as shown in Fig. 14b compared to a. This may be explained by the fact that higher cutting temperature and larger stress were produced as the increase of cutting speed and feed rate.

## 4 Conclusion

A series of dry drilling trials of alloy Ti6Al4V have been conducted in this paper, aiming to analyze thrust force, burr formation mechanism, quality of drilling holes, chips formation and surface integrity. From obtained results, several conclusions can be summarized as follows.

- Thrust force variation was corresponded to the penetrating depth of the twist drill into the workpiece. It increased rapidly with respect to feed rate, which was increased by 2.5 times when the feed was increased from 0.05 to 0.13 mm/r as a constant cutting speed of 40 m/min.
- Three types of burrs were classified based on the fracture location and burr formation mechanism was analyzed. The fracture of burr was determined by comparing the strain at the drill point with that along the exit edge of the hole.
- The shape and the size of chips are strongly influenced by the selection of the feed rate. In order to ensure drilling and

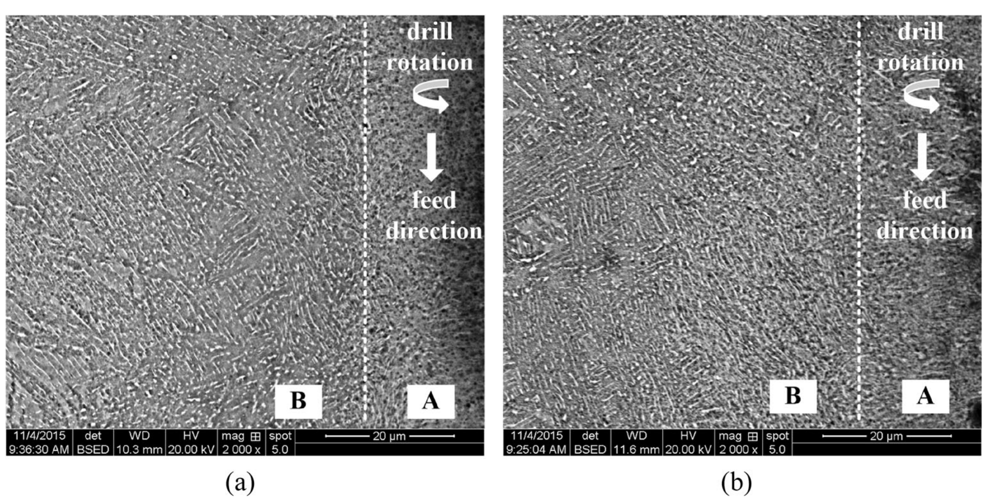


**Fig. 14** SEM micrograph of the material workpiece for different cutting parameters. **a** $v_c$ = 26 m/min, $f$ = 0.05 mm/r. **b** $v_c$ = 55 m/min, $f$ = 0.2 mm/r

riveting in an automated assembly, the chips should be broken into segments and should not to be attached to the body of drill. The experimental results indicate that drilling at a feed rate of 0.2 mm/r gives broken segmental chips.

- Surface roughness was considerably smoother under high cutting speed and low feed rate in comparison to low cutting speed and high feed rate. Some parallel grooves were obtained in hole surface at low cutting speed. There are two distinct regions according to the feature of micro-structure, named region A and region B. In region A which is closer to the drilled hole surface, the grains were refined obviously, while the grains in region B were deformed and oriented along the feed rate direction.

**Acknowledgements** The authors acknowledge the financial support of the National Natural Science Foundation of China (Grant No. 51305236) to carry out this research work.

## References

1. Shetty PK, Shetty R, Shetty D, Rehaman NF, Jose TK (2014) Machinability study on dry drilling of titanium alloy Ti-6Al-4V using L9 orthoganal array. Procedia Materials Science 5:2605–2614
2. Zhang PF, Churi NJ, Pei ZJ, Treadwell C (2008) Mechanical drilling processes for titanium alloys: a literature review. Mach Sci Technol 12:417–444
3. Sun J, Guo YB (2008) A new multi-view approach to characterize 3D chip morphology and properties in end milling titanium Ti–6Al–4V. Int. J. Tools Manuf. 48:1486–1494
4. Lei S, Liu WJ (2002) High-speed machining of titanium alloys using the driven rotary tool. Int. J. Tools Manuf. 42:653–661
5. Hsu I, Tsao CC (2008) Study on the effect of frequency tracing in ultrasonic-assisted drilling of titanium alloy. Int Journal Adv Manuf Technol 43(1–2):127–135
6. Bi S, Liang J (2010) Experimental studies and optimization of process parameters for burrs in dry drilling of stacked metal materials. Int Journal Adv Manuf Technol 53(9–12):867–876
7. Ren N, Jiang L, Liu D, Lv L, Wang Q (2014) Comparison of the simulation and experimental of hole characteristics during nanosecond-pulsed laser drilling of thin titanium sheets. Int Journal Adv Manuf Technol 76(5–8):735–743
8. Cantero JL, Tardío MM, Canteli JA, Marcos M, Miguélez MH (2005) Dry drilling of alloy Ti–6Al–4V. Int. J. Tools Manuf. 45:1246–1255
9. Li R, Hegde P, Shih AJ (2007) High-throughput drilling of titanium alloys. Int. J. Tools Manuf. 47:63–74
10. Dornfeld DA, Kim JS, Dechow H, Hewson J, Chen LJ (1999) Drilling burr formation in titanium alloy, Ti-6AI-4V. CIRP Ann–Manuf Technol 48:73–76
11. Abdelhafeez AM, Soo SL, Aspinwall DK, Dowson A, Arnold D (2015) Burr formation and hole quality when drilling titanium and aluminium alloys. Procedia CIRP 37:230–235
12. Cao Z, Liu Z, Wang X, Qiu M, Hui Z (2015) Monopulse electrical discharge machining ablation drilling technology for Ti-6Al-4V titanium alloy. Int Journal Adv Manuf Technol. doi:10.1007/s00170-015-8169-9
13. Bermingham MJ, Palanisamy S, Morr D, Andrews R, Dargusch MS (2014) Advantages of milling and drilling Ti-6Al-4V components with high-pressure coolant. Int Journal Adv Manuf Technol 72(1–4):77–88
14. Bi S, Liang J (2010) Robotic drilling system for titanium structures. Int Journal Adv Manuf Technol 54(5–8):767–774
15. Shyha IS, Soo SL, Aspinwall DK, Bradley S, Perry R, Harden P, Dawson S (2011) Hole quality assessment following drilling of metallic-composite stacks. Int. J. Tools Manuf. 51:569–578
16. Denkena B, Boehnke D, Dege JH (2008) Helical milling of CFRP–titanium layer compounds, CIRP J. Manuf Sci Technol 1:64–69
17. Ramulu M, Young P, Kao H (1999) Drilling of graphite/bismaleimide composite material. J Mater Eng Perf 8:330–338
18. Pawar OA, Gaikhe YS, Tewari A, Sundaram R, Joshi SS (2015) Analysis of hole quality in drilling GLARE fiber metal laminates. Compos Struct 123:350–365
19. Bono M, Ni J (2001) The effects of thermal distortions on the diameter and cylindricity of dry drilled holes. Int. J. Tools Manuf. 41:2261–2270
20. Brinksmeier E, Pecat O, Rentsch R (2015) Quantitative analysis of chip extraction in drilling of Ti6Al4V. CIRP Annals–Manuf Technol 64:93–96
21. Prasanna J, Karunamoorthy L, Venkat Raman M, Prashanth S, Raj Chordia D (2014) Optimization of process parameters of small hole dry drilling in Ti–6Al–4V using Taguchi and grey relational analysis. Measurement 48:346–354
22. Ko S, Lee J (2001) Analysis of burr formation in drilling with a new-concept drill. J Mater Process Technol 113:392–398
23. Ko S, Chang J, Yang G (2003) Burr minimizing scheme in drilling. J Mater Process Technol 140:237–242
24. Nouari M, List G, Girot F, Géhin D (2005) Effect of machining parameters and coating on wear mechanisms in dry drilling of aluminium alloys. Int J Tools Manuf 45:1436–1442
25. Zhu ZJ, Sun J, Li JF, Huang PL (2016) Investigation on the influence of tool wear upon chip morphology in end milling titanium alloy Ti6Al4V. Int J Adv Manuf Technol 83:1477–1485
26. Zitoune R, Krishnaraj V, Collombet F (2010) Study of drilling of composite material and aluminium stack. Compos Struct 92:1246–1255